

# Electrical properties in $\text{WO}_3$ doped $\text{Bi}_4\text{Ti}_3\text{O}_{12}$ materials

T. Jardiel\*, A.C. Caballero, M. Villegas

*Department of Electroceramics, Instituto de Cerámica y Vidrio (CSIC), Madrid 28049, Spain*

Available online 29 March 2007

## Abstract

Electrical conductivity decrease observed in BIT-based materials doped with  $\text{W}^{6+}$  is consistent with a lowering of both oxygen vacancies and hole concentration. The dielectric anomaly observed in BIT at temperatures below  $T_c$  decreases and finally disappears with the donor doping. Following the same trend, dielectric losses fall when the amount of dopant increases and remain in low values up to high temperatures. Compared to undoped BIT, substitution of  $\text{Ti}^{4+}$  by  $\text{W}^{6+}$  leads to a decrease of 2–3 orders of magnitude in the electrical conductivity. The average activation energy for the electrical conductivity depends on the microstructure, specifically on the aspect ratio (length/thickness) of the plate-like grains. This is because the conduction mechanism in the *ab* planes is different to that of the *c*-axis, mixing ionic and p-type conductivity, respectively.

© 2007 Elsevier Ltd. All rights reserved.

**Keyword:**  $\text{Bi}_4\text{Ti}_3\text{O}_{12}$  ceramics; Platelets; Electrical properties; Impedance; Electrical conductivity

## 1. Introduction

Bismuth titanate, BIT, is one of the most studied compounds among the bismuth-based layered ceramics because of its ferroelectric properties and lead-free nature. It is a high temperature ferroelectric ceramic ( $T_c = 650^\circ\text{C}$ ) with useful properties for optical memory, high temperature piezoelectric and electro-optic devices.<sup>1,2</sup>

Structure of  $\text{Bi}_4\text{Ti}_3\text{O}_{12}$  can be described as formed by three unit cells of  $(\text{BiTiO}_3)^{2-}$  with perovskite-like structure ( $m=3$ ), interleaved with  $(\text{Bi}_2\text{O}_2)^{2+}$  layers.<sup>3</sup> This structure promotes a plate-like morphology, with platelets growing preferentially in the *ab* plane. The main component of the spontaneous polarization ( $P_s \approx 50 \mu\text{C}/\text{cm}$ ) lies in the *ab* plane.<sup>4</sup> However, the electrical conductivity is also very high in this plane,<sup>5</sup> and as a consequence BIT ceramics are very difficult to pole. Consequently the decrease of electrical conductivity is one of the main goals of BIT investigations.

Regarding to its electrical transport properties, the mechanism of conduction in BIT is not clear yet. As it has been shown, the aspect ratio of the platelets plays a critical role on the conductivity of BIT ceramics.<sup>6</sup> Donor doping with  $\text{Nb}^{5+}$ ,  $\text{V}^{5+}$  or  $\text{W}^{6+}$ , significantly decreases the conductivity in BIT-based ceramics indicating that the conductivity is p-type.<sup>7–11</sup>

Recent publications point out that charge transport in BIT polycrystalline specimens has electronic and ionic components.<sup>12,13</sup> The electronic conductivity is p-type and is dominant along *c*-axis. On the other hand, the ionic conductivity is due to oxygen vacancies and takes place predominantly in the *ab* plane.

Within this background, the main objective of the present contribution is to analyze the electrical properties of W (VI)-doped  $\text{Bi}_4\text{Ti}_3\text{O}_{12}$  materials.

## 2. Experimental procedure

Undoped BIT ceramics were prepared by a chemical route, using the hydroxide coprecipitation method. Titanium tetrabutoxide  $\text{Ti}(\text{C}_4\text{H}_9\text{O})_4 \cdot \text{C}_4\text{H}_9\text{OH}$  (Alfa Aesar),  $\text{Bi}(\text{NO}_3)_3 \cdot 5\text{H}_2\text{O}$  (Riedel de Hën) and  $\text{W}(\text{C}_2\text{H}_5\text{O})_6$  (Alfa Aesar) were used, respectively, as  $\text{TiO}_2$ ,  $\text{Bi}_2\text{O}_3$  and  $\text{WO}_3$  precursors. Experimental details are reported elsewhere.<sup>7</sup> The BIT coprecipitated powders were air-calcined at  $650^\circ\text{C}$  for 1 h. Doping was done by particle surface coating using  $\text{W}(\text{C}_2\text{H}_5\text{O})_6$  as a source for W(VI). Ceramic powders with a general formula  $\text{Bi}_4\text{Ti}_3\text{W}_x\text{O}_{12+3x}$  with  $x=0, 0.02, 0.05, 0.08$  and  $0.15$  were obtained. BIT-based powders were uniaxially pressed into disks (250 MPa) and sintered in air at temperatures between 800 and  $1150^\circ\text{C}$  (2 h soaking time).

Apparent density of the sintered samples was measured by the Archimedes method. Sintered samples were characterized by powder XRD diffraction (Siemens D5000). The microstructure of the sintered compacts was studied by Scanning Electron

\* Corresponding author.

E-mail address: [jardiel@icv.csic.es](mailto:jardiel@icv.csic.es) (T. Jardiel).

Microscopy (Carl Zeiss DSM 950) on polished and thermally etched surfaces. Electrical measurements were done on Ag electroded disks of 1 mm thickness. Dielectric characterization was performed using a HP4192A impedance analyzer in the temperature range 25–750 °C. AC conductivity was analyzed by complex impedance spectroscopy in a temperature range from 400 to 750 °C.

### 3. Results and discussion

Sintering behaviour of BIT-based ceramics was modified by the amount of dopant (Fig. 1a). Maximum density occurs at higher temperature as the amount of  $W^{6+}$  increases. This change, due to the presence of  $WO_3$  surrounding BIT particles, points out to  $W^{6+}$  being the rate controlling species of diffusion. Anyway, high density values are reached for all the materials under study. Fig. 1b shows the XRD patterns of BIT-based materials sintered at maximum density temperature. No secondary phases are observed in any composition. Differences measured in the intensities of the peaks corresponding to the (001) family are caused by the growth of the platelets in the *ab* plane for compositions with lower level of dopant.

Aspect ratio behaviour is shown in Fig. 2. It is clearly observed that the higher the amount of tungsten the lower the

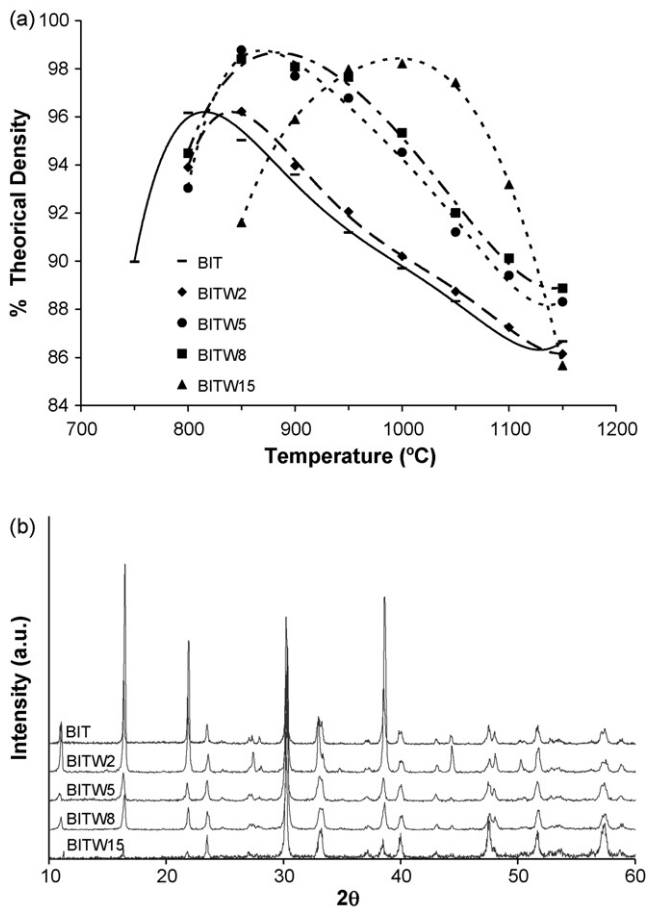


Fig. 1. (a) Theoretical density as a function of temperature for BIT-based materials. (b) XRD patterns for the different materials sintering at temperature of maximum density. All peaks corresponding to the  $Bi_4Ti_3O_{12}$  phase.

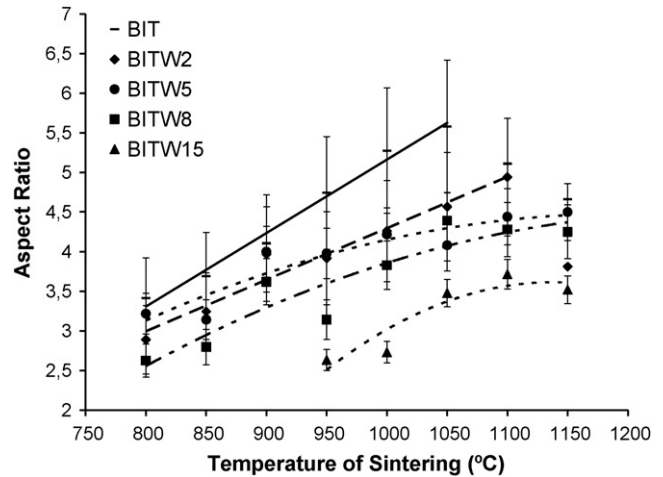


Fig. 2. Aspect ratio as a function of temperature for BIT-based materials.

aspect ratio for a given temperature. The same aspect ratio can be reached increasing the sintering temperature together with the dopant concentration. This point is relevant since comparing samples with very different aspect ratio can be meaningless from the point of view of electrical transport.

Fig. 3 depicts the evolution of the dielectric constant and the dielectric losses as a function of temperature at 1 MHz. It is observed that the dielectric constant decreases when increasing  $WO_3$  amount up to  $x = 0.08$ , but the most interesting effect takes place at low temperatures where the curve corresponding to pure BIT ceramics shows a different shape at temperatures around 550 °C. This dielectric anomaly is always observed in undoped BIT, both in single crystals and in ceramics. Its appearance has been attributed to different phenomena but in recent works the most accepted explanation is the ion-jump relaxation, specifically by oxygen ion motion.<sup>10</sup> Such anomaly is not observed in the rest of the curves, which is due to the  $W^{6+}$  doping.

Fig. 3 also shows that for  $x \leq 0.08$  the Curie temperature decreased slightly with the amount of dopant. This is a consequence of the substitution of  $W^{6+}$  in the  $Ti^{4+}$  lattice site, which promotes a slightly diminution of the crystal lattice distortion.<sup>14</sup> Moreover, in Fig. 3b it is observed that the dielectric losses decreased drastically with the addition of  $WO_3$ , especially when  $x \leq 0.08$ . Then they remain in very low values up to very high temperatures ( $\approx 650$  °C). This behaviour in dielectric losses as well as the disappearance of the dielectric anomaly, points to a decrease in both the p-type electrical conductivity and the oxygen vacancies motion.

Another feature detected in this same figure is the presence of a second peak in the curve of BITW15 composition, observed at temperatures above the transition temperature of BIT ( $\sim 675$  °C). This second transition is due to the presence of a secondary Aurivillius-type phase,  $Bi_6Ti_3WO_{18}$ , with its ferroelectric-paraelectric transition at 705 °C. The presence of this secondary phase, which is always formed when preparing BITW15 composition,<sup>15</sup> was confirmed by X-ray diffraction. As can be observed in Fig. 4, peaks corresponding to this phase are detected at temperatures above 1150 °C. At lower temperatures

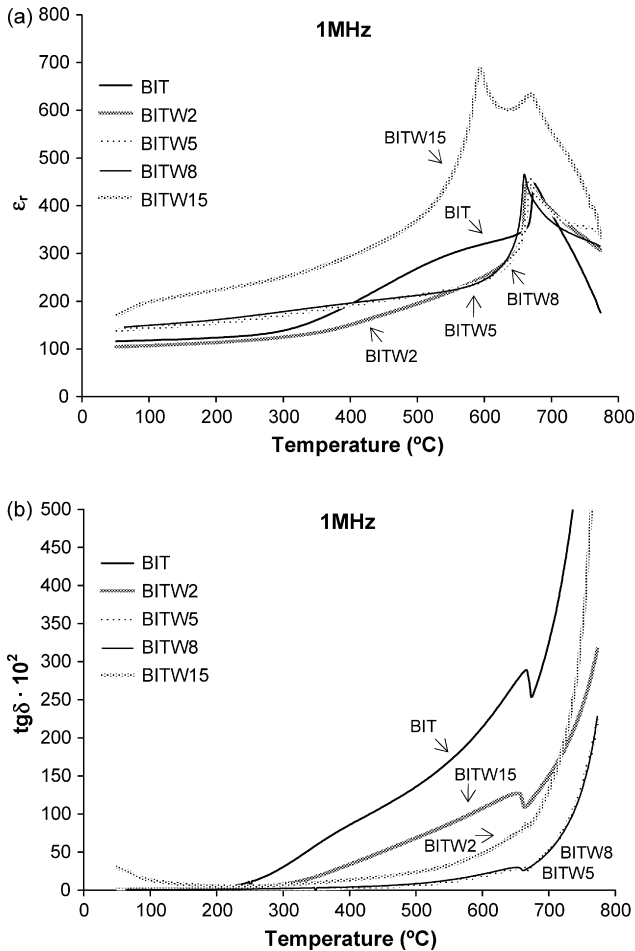


Fig. 3. (a) Dielectric constant and (b) dielectric losses vs. temperature at 1 MHz for BIT-based materials sintered at 950 °C.

it is assumed that this phase interacts with pure BIT to form a regular intergrowth compound;<sup>16</sup> this one is responsible of the shifting in the ferroelectric transition temperatures of BITW15 composition toward lower temperatures (around 40 °C), however, it cannot be detected by XRD since its pattern is close to that of pure BIT. At 1150 °C this intergrowth compound decomposes and melts to give the  $\text{Bi}_6\text{Ti}_3\text{WO}_{18}$  phase that we observe in XRD of Fig. 4.

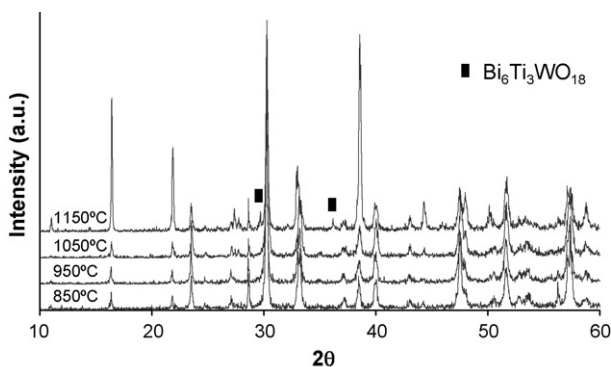


Fig. 4. XRD patterns for BITW15 composition at different sintering temperatures.

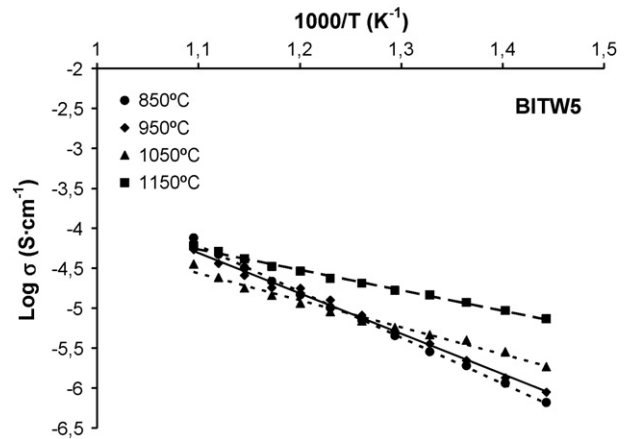


Fig. 5. Arrhenius plots of the electrical conductivity for BITW5 samples at different sintering temperatures.

Electrical conductivity of BIT polycrystals was analyzed by complex impedance spectroscopy in a frequency range from 0.1 kHz to 10 MHz and for temperatures ranging from 400 to 650 °C. The fitting of the impedance diagrams gave the activation energies as well as bulk conductivities, as a function of temperature. According to this, Fig. 5 shows the Arrhenius plots of the bulk electrical conductivity for BITW5 compacts sintered at different temperatures. All samples present analogous conductivity but the slope of the curves changes with the sintering temperature. As mentioned in the introduction, recent publications describe the conductivity in BIT as a mixture between ionic and electronic conduction,<sup>12,13</sup> therefore the calculated activation energy comes from the sum of the activation energies of both mechanisms. Since evaluated samples contain the same level of dopant, changes in the global activation energies should be attributed to differences in the aspect ratio of the platelets. This is so because *ab* plane and *c*-direction exhibit different conduction mechanisms.<sup>12,13</sup>

Arrhenius plots of the electrical conductivity for the BIT-based ceramics sintered at 950 °C are showed in Fig. 6. As expected, bulk electrical conductivity decreased with the amount of donor dopant. BITW5 and BITW8 compositions presented

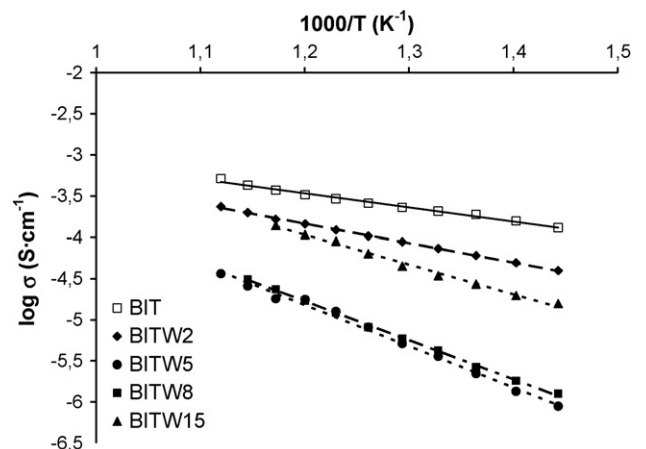


Fig. 6. Arrhenius plots of the electrical conductivity for samples sintered at 950 °C.

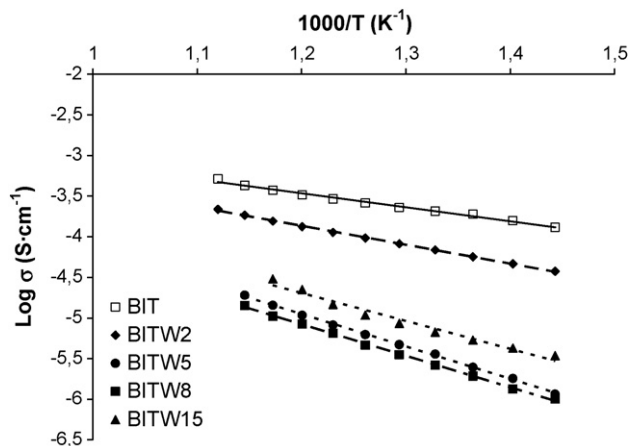
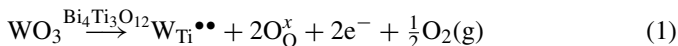


Fig. 7. Arrhenius plots of the electrical conductivity for samples with similar aspect ratio ( $lt \sim 3.7$ ).

similar activation energy and also a similar conductivity, with a decrease of about 2–3 order of magnitude with regards to pure BIT. This behaviour indicates that the incorporation level of  $W^{6+}$  in the BIT lattice is similar in both compositions, pointing that the solid solution limit is around 5 mol% of  $WO_3$ . Electrical conductivity increased in BITW15 sample due to the presence of  $Bi_6Ti_3WO_{18}$  secondary phase, which exhibits a higher conductivity than BIT.<sup>17</sup> The decrease of electrical conductivity by donor doping is thought to be produced by the reduction of ionic conductivity (oxygen vacancies) and electronic conductivity (holes) due to the following defects compensation mechanisms:



Therefore, other factor contributing to the decrease in conductivity is the morphology of the platelets. As can be observed in Fig. 2, the aspect ratio (length/thickness) of the grains decreases with the amount of dopant, which contributes to the reduction in the conductivity. In order to eliminate the influence of the morphology of the platelets, the conductivity of samples with similar aspect ratio was compared (Fig. 7). The most important effect is that the activation energy does not change among the curves, indicating that the average conductivity (ionic + electronic) remains constant. Recent reports give evidence that the principal carrier along  $ab$  plane is oxygen vacancies while p-type conduction is dominant along  $c$ -axis.<sup>12,13</sup> Therefore, the aspect ratio of the platelets reflects a balance between  $ab$  plane and  $c$ -axis oriented directions and, since each orientation has a predominant charge transport mechanism, the average activation energy changes with the aspect ratio. On the other hand, comparing samples with similar aspect ratio electrical conductivity was reduced in about 2–3 orders of magnitude for BITW5 and BITW8 compositions. Thus, the decrease of the conductivity is related to the effect of donor doping and temperature, indicating again that  $WO_3$  solid solution limit into BIT lattice is around  $x \sim 0.05$ . However, as it has been dis-

cussed above, no further reduction in the electrical conductivity is obtained for composition with  $x = 0.15$ .

#### 4. Conclusions

Incorporation of  $W^{6+}$  into the BIT lattice decreases both the amount of oxygen vacancies and holes, leading to a diminution in the ionic and electronic conductivities. This reduction in the conductivity with the donor doping, specifically that of oxygen vacancies, also promotes the decrease and lately disappearance of the dielectric anomaly observed in BIT at temperatures below  $T_c$ . For the same reason, dielectric losses decrease with the amount of dopant, remaining in low values up to high temperatures.

In compositions with 5 or 8 mol% of  $WO_3$  the electrical conductivity decreases up to 2–3 orders of magnitude respect to the undoped BIT. This result indicates that the solid solution limit of  $W^{6+}$  into the BIT lattice is around  $x \sim 0.05$ .

Finally the aspect ratio of the platelets also has influence on the activation energies since every orientation in the platelets has a predominant charge transport mechanism. Therefore the average activation energy of the conductivity changes with the aspect ratio of the plate-like grains.

#### References

- Subbarao, E. C., A Family of ferroelectric bismuth compounds. *J. Phys. Chem. Solids*, 1965, **23**, 665–676.
- Scott, J. F. and Araujo, C. A., Ferroelectric memories. *Science*, 1989, **246**, 1400.
- Aurivillius, B., Mixed bismuth oxides with layer lattices II. *Ark. Kemi.*, 1949, **1**, 499–512.
- Cummings, S. E. and Cross, L. E., Electrical and optical properties of ferroelectric  $Bi_4Ti_3O_{12}$  single crystals. *J. Appl. Phys.*, 1968, **39**, 2268–2274.
- Fouskova, A. and Cross, L. E., Dielectric properties of bismuth titanate. *J. Appl. Phys.*, 1970, **41**, 2834–2838.
- Villegas, M., Caballero, A. C., Moure, C., Durán, P. and Fernández, J. F., Factors affecting the electrical conductivity of donor-doped  $Bi_4Ti_3O_{12}$  piezoelectric ceramics. *J. Am. Ceram. Soc.*, 1999, **82**, 2411–2416.
- Villegas, M., Jardiel, T. and Farías, G., Sintering and electrical properties of  $Bi_4Ti_{2.95}W_xO_{11.9+3x}$  piezoelectric ceramics. *J. Eur. Ceram. Soc.*, 2004, **24**(6), 1025–1029.
- Villegas, M., Jardiel, T., Caballero, A. C. and Fernández, J. F., Sintering and electrical properties of bismuth titanate based ceramics with secondary phases. *J. Electroceram.*, 2004, **13**, 543–548.
- Lopatin, S. S., Lupeiko, T. G., Vasil'tsova, T. L., Basenko, N. I. and Berlizev, I. M., Properties of bismuth titanate ceramics modified with group V and VI elements. *Inorg. Mater. (Eng. Trans.)*, 1989, **24**, 1551–1554.
- Shulman, H., Damjanovic, D. and Setter, N., Niobium doping and dielectric anomalies in bismuth titanate. *J. Am. Ceram. Soc.*, 2000, **83**(3), 528–532.
- Zhang, L., Suchuan, Z., Zheng, L., Guorong, L. and Qingrui, Y., Effects of donor doping on microstructure and electrical properties of bismuth layer-structured  $Bi_4Ti_3O_{12}$  ceramics. *Key Eng. Mater.*, 2005, **280–283**, 259–262.
- Takahashi, M., Noguchi, Y. and Miyayama, M., Effects of V-doping on mixed conduction properties of bismuth titanate single crystals. *Jpn. J. Appl. Phys.*, 2003, **42**, 6222–6225.
- Takahashi, M., Noguchi, Y. and Miyayama, M., Electrical conduction mechanism in  $Bi_4Ti_3O_{12}$  single crystal. *Jpn. J. Appl. Phys.*, 2002, **41**, 7053–7056.

14. Takenaka, T. and Sakata, K., Electrical properties of grain-oriented ferroelectric ceramics in some lanthanum modified layer-structure. *Ferroelectrics*, 1981, **38**, 769–772.
15. Jardiel, T., Caballero, A. C., Villegas, M., Valant, M., Jancar, B. and Suvorov, D., Equilibrium phases in the system  $\text{Bi}_2\text{O}_3\text{--TiO}_2\text{--WO}_3$ . *J. Eur. Ceram. Soc.*, 2006, **26**(14), 2931–2935.
16. Luo, S., Noguchi, Y., Miyayama, M. and Kudo, T., Rietveld analysis and dielectric properties of  $\text{Bi}_2\text{WO}_6\text{--Bi}_4\text{Ti}_3\text{O}_{12}$  ferroelectric system. *Mater. Res. Bull.*, 2001, **36**, 531–540.
17. Jardiel, T., Caballero, A. C., De Frutos, J. and Villegas, M., Sintering electrical properties of  $\text{Bi}_6\text{Ti}_3\text{WO}_{18}$  ceramics. *Ferroelectrics*, 2006, **336**, 145–152.